PHYSICAL REVIEW C VOLUME 19, NUMBER 2 FEBRUARY 1979

Photonuclear yields of the ^{237}Pu fission isomers

W. Günther, K. Huber, U. Kneissl, and H. Krieger
Institut für Kernphysik, Strahlenzentrum, Justus-Liebig-Universität, 6300 Giessen, West Germany

H. J. Maier
Ludwig-Maximilian-Universität, 8000 München, West Germany
(Received 13 June 1978, revised manuscript received 28 September 1978)

The half-lives and yield ratios Y_{iso}/Y_{prompt} for the two ^{237}Pu fission isomers have been investigated in the photonuclear reaction $^{239}Pu(\gamma,2n)$. The observed half-lives ($t_{1/2} = 77 \pm 16$ ns, 1050 ± 400 ns) agree well with the data from particle induced fission. The measured yield ratios were $(Y_{iso}/Y_{prompt})_f^{short} = (6.4 \pm 1.7) \times 10^{-6}$ and $(Y_{iso}/Y_{prompt})_f^{long} = (0.83 \pm 0.22) \times 10^{-6}$. From a statistical model analysis of the isomeric fission yield ratio ($Y_{short}/Y_{long} = 7.7 \pm 2.9$) a spin assignment of the two shape isomers was attempted. The analysis provided, in the context of the statistical model, the most probable spin values $I = 11/2$ for the exicted, long lived state and $I = 5/2$ for the short lived ground state in the second minimum of ^{237}Pu. Comparing these spin values with single particle calculations, we tend to classify the excited state as the $[615]_{11/2+}$ Nilsson orbit and the short lived state as the $[862]_{5/2+}$ state.

[NUCLEAR REACTIONS $^{239}Pu(\gamma,2n)$, bremsstrahlung 45 MeV; measured $t_{1/2}$, Y_{iso}/Y_{pr} for $^{237}Pu^{m1,m2}$ deduced isomeric ratio, spins.]

I. INTRODUCTION

The large deformation of fission isomers was quantitatively demonstrated by the experiments of Specht *et al.*[1] and Habs *et al.*,[2] who measured the energies and lifetimes of rotational states in the second well of the potential energy surface. The investigation of excited states in the second minimum is of fundamental interest, since more detailed information concerning the strongly deformed nucleus can be extracted from such experiments.

Besides collective bands, low lying single particle excitations are possible in odd nuclei. The identification and classification of single particle levels in the second well represent a crucial test of single particle models and their extrapolation to large deformations and, consequently, of the whole Strutinsky procedure. As is well known, these shell model extrapolations are used within Strutinsky's hybrid model[3,4] to calculate the deformation-dependent shell corrections, which generate the double humped fission barrier of the actinides.

If the γ decay of excited single particle levels in the second well is hindered by spin-selection rules, these spin isomers are accessible to experiments. The most thoroughly investigated nucleus with two fissioning isomers in the second well is ^{237}Pu ($T_{1/2} \approx 100$ ns and 1.1 μs, respectively).[5-14] These Pu isomers can be populated with sufficiently high cross sections in $(\alpha, 2n)$ and $(d, 2n)$ reactions on available targets (^{235}U, ^{237}Np). From excitation function measurements[12] it was concluded that the long-lived state lies about 0.3 MeV above the 100 ns level. Consequently, the short-lived state was ascribed to the ground state in the second well and the 1.1 μs level is assumed to correspond to a single particle excitation of the odd neutron.

In order to identify the isomeric states as certain Nilsson levels the spin and K values have to be determined. A first spin assignment for the ^{237}Pu isomers was attempted by Vandenbosch and co-workers,[11] who had measured the relative population of both isomers in $(\alpha, 2n)$ and $(d, 2n)$ reactions for different angular momentum transfer into the compound system. The authors conclude from a conventional statistical model analysis of their results that the 1.1 μs state has the higher spin. However, uncertainties exist in this analysis, due to the unknown branching ratio of the isomeric decay, which possibly give rise to an underestimation of the shortlived isomeric yield. Further deficiencies arise from the statistical formalism. Although no definite spin determination was possible by this method, a spin combination $\frac{11}{2} - \frac{5}{2}$ for the isomeric pair could be favored, a result which is in disagreement with the analysis of Hamamoto *et al.*[15] based on fragment angular distribution and g-factor measurements.[16,17] Unfortunately, the results of these measurements, using a spin alignment in (α, xn) reactions must be regarded as very tentative since these experiments are partially inconsistent and not reproducible.[18,19] These experiments are sensitive to approximations applied to the analysis of anisotropies and to problems of conservation of the spin alignment for sufficiently long time.

The aim of our experiments was to measure the relative population of the ^{237}Pu isomers in a photonuclear reaction via the ^{239}Pu $(\gamma, 2n)$ process. This type of reaction represents a significant extension of the range of transferred angular momentum covered by particle induced reactions. Owing to the predominant dipole excitations in photonuclear reactions, the angular momentum transfer is low in contrast to (α, xn) or (d, xn) reactions. This leads to a favored population of low spin states. Therefore, a (γ, xn) isomeric ratio measurement should be especially sensitive to the identification of the high spin state of the two ^{237}Pu isomers. It is evident that the conclusions from these measurements based on a statistical model analysis are affected with the same restrictions as those from particle induced reaction data.[11] However, in combination with the $(\alpha, 2n)$ and $(d, 2n)$ data, a more reliable spin assignment should be possible. The comparison with different theoretical calculations[20–23,15] of the Nilsson orbitals provides an important test of these models and may enable reliable extrapolations of these calculations to large deformations and other mass regions.

II. EXPERIMENTAL PROCEDURE

The experiments were performed at the bremsstrahlung facility of the Giessen electron linac. The experimental setup is described in more detail in Ref. 24. The fission fragments were detected by two large-area surface barrier detectors (900 mm^2). The ^{239}Pu-target assembly consisted of two 250 μg/cm^2 layers of ^{239}Pu (diameter 2 cm, purity 99.99%) each evaporated on a 30 μg/cm^2 carbon backing. The two Pu targets were glued face to face in a 1 mm distance, in order to reduce a possible Pu contamination of the detectors and the vacuum chamber. Time distributions were measured by pulsed beam techniques and conventional electronics as described in Ref. 25. We used two different linac pulse widths in order to optimize the population of each of the two isomeric states. In particular, a large time range was covered in the measurements in order to estimate small long-lived background contaminations (e.g. from thermal neutron capture). The beam conditions are summarized in Table I.

In order to analyze the measured time distributions, these are plotted in a 2-logarithmic time scale.[26] In this kind of graph an exponential decay shows an intensity distribution with its maximum value at the half-life. Obviously, this representation is advantageous for display of a decay curve with two or more time components. The intensities and half-lives were determined by least-squares fits to the intensity distributions. Details are described in Ref. 26.

III. RESULTS

Figure 1 shows the time distributions measured in the runs with 50 ns beam pulses. The four curves correspond to different delay times (6–24 ns) with respect to the beam burst. In the ^{2}log-time representation each of the two maxima corresponds to one half-life. The positions of the maxima remain constant with respect to the time axis for all four fits and yield half-lives of (11 ± 6) ns and (80 ± 20) ns, respectively; the amplitude of the short-lived component decreases consistently with increasing delay time to the beam burst. The 80 ns amplitude, of course, remains nearly constant for the short delay of only 24 ns. This is regarded as a proof of the reliability of our least-squares fits results.

Figure 2 shows a fit to our data from the long beam pulse experiments (≈1000 ns). The first of the three bumps in the time distribution ($t_{1/2} = 72 \pm 26$ ns) should correspond to the (80 ± 20) ns component. The second bump ($t_{1/2} = 1050 \pm 400$ ns) may be ascribed to an excitation of the 1.1 μs isomer. The increase of the intensity distribution at longer times is caused by a small, nearly constant background. The successive doubling of the time intervals in the ^{2}log-time scale leads to the increase of the background intensity by 2^n for the nth interval. The long-lived maximum is believed to correspond to neutron moderation in the shielding of our experimental setup.

The importance of covering a large time range is easily appreciated with respect to a reliable long-lived background correction of the data (time

TABLE I. Experimental conditions in the pulsed beam experiments.

Pulse length (ns)	Repetition rate (s^{-1})	Time range (μ s)	Bremsstrahlung end point energy (MeV)
50	1000	5	45
≈1000	400	≈70	45

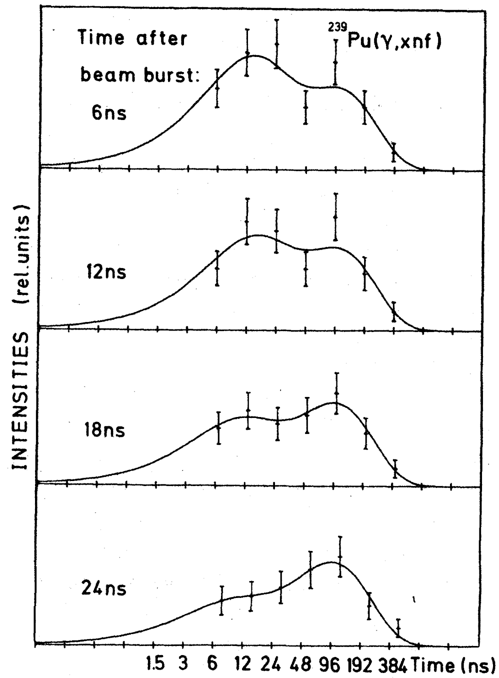

FIG. 1. Fission fragment time distributions from the short beam pulse experiments (^{2}log-time-scale representation).

range about 70 μs for the long beam pulse experiments). In Table II the results of about 6 weeks of beam time are summarized. In the experiments with short beam bursts (50 ns) we observed a half-life of (80 ± 20) ns with an isomeric to prompt fission ratio of $(6.2 \pm 1.8) \times 10^{-6}$. Owing to the agreement between the measured half-life and previous results, this component is ascribed to the ground state in the second well of ^{237}Pu. The (11 ± 6) ns component may possibly correspond to an excitation of the two quasiparticle state in ^{238}Pu,[31] which could be populated in a (γ, n) reaction. However, this must be investigated in further experiments on ^{240}Pu. In our experiments with long beam pulses (1000 ns) a (72 ± 26) ns component was also observed corresponding to the ground state in the second well of ^{237}Pu. Additionally, a long-lived component (1050 ± 400 ns) with a relatively low isomeric to prompt fission ratio of $(0.83 \pm 0.22) \times 10^{-6}$ has been detected. This half-life is consistent with the decay of the excited single neutron state in the second well of ^{237}Pu. The isomeric ratio, i.e., the yield ratio for the population of the short-lived and the long-lived state, was determined to be $Y_{\mathrm{short}}/Y_{\mathrm{long}} = 7.7 \pm 2.9$.

IV. DISCUSSION

A. Comparison of the half-lives with previous results

In Table III the results of previous (α, 2n) and (d, 2n) experiments are summarized. A good agreement between these and our measured half-lives for both isomers is observed. The result of an earlier ^{239}Pu (γ, xn) experiment of Tamain *et al.*,[27] who observed a half-life of ≈500 ns with a relative population of $Y_{\mathrm{iso}}/Y_{\mathrm{pr}} \approx 0.7 \times 10^{-5}$, could not be confirmed by our experiments.

B. Isomeric yield ratio and spin assignments

In this section we attempt spin assignments applying the conventional Huizenga-Vandenbosch statistical model analysis[28,29] to our measured isomeric yield ratios. At first, the (γ, 2n) result is compared with (α, 2n) and (d, 2n) data reported by Vandenbosch *et al.*[11] The most important difference between these three reactions is the different deposition of angular momentum into the compound nucleus system. In the (α, 2n) reactions with 27

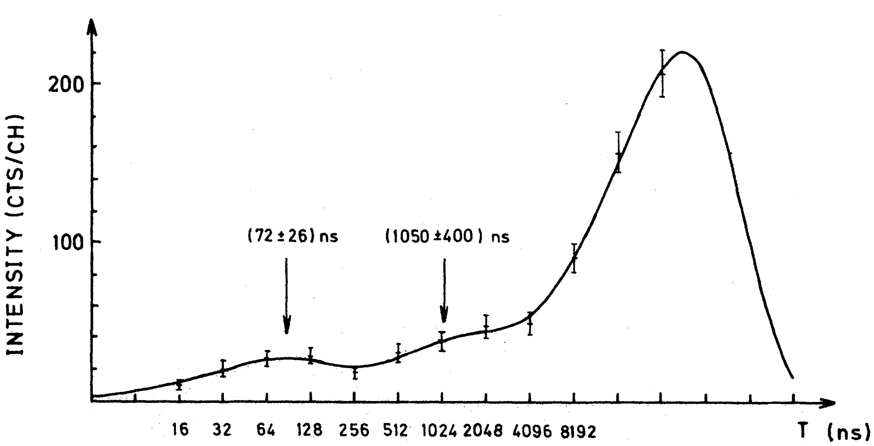

FIG. 2. Fission fragment time distribution from the long beam pulse experiment (^{2}log-time-scale representation).

TABLE II. Results.

Pulse length (ns)	$T_{1/2}$(ns)	$Y_{iso}/Y_{pr}\times 10^6$	$N_{pr}\times 10^{-6}$	Assignment
50	80 ± 20	6.2 ± 1.8	21.4	$^{237}Pu^{m1}$
	11 ± 6	···	21.4	$^{238}Pu^{m}$(?)
	long–lived	< 1.5	21.4	
1000	72 ± 26	10.9 ± 8.5	236.0	$^{237}Pu^{m1}$
	1050 ± 400	0.83 ± 0.22	···	$^{237}Pu^{m2}$

and 24 MeV α particles the mean squared spin value $\overline{J_c^2}$ of the compound nucleus is $53\hbar^2$ and $27\hbar^2$, respectively; for the $(d, 2n)$ reaction at 12 MeV $\overline{J_c^2}$ is about $15\hbar^2$. For a $(\gamma, 2n)$ reaction, however, this value amounts only to about $1.6\hbar^2$. In Fig. 3 we show a plot from Ref. 11 of the statistical model calculations of $\sigma_{low}/\sigma_{high}$ as a function of $\overline{J_c^2}$ for different spin combinations of the two isomers. The curves were extrapolated (dashed lines) to low $\overline{J_c^2}$ values using our program for the isomeric ratio analysis,[30] which is based on the same statistical model assumptions as used in Ref. 11, just modified for photonuclear reactions. The experimental yield ratio Y_{short}/Y_{long} decreases for higher $\overline{J_c^2}$ values and spin combinations, such that the higher spin is ascribed to the long-lived state. This is explained by the relative increase in population of the high spin state with increasing angular momentum in the compound system. For a reversed spin assignment the curves show an opposite slope (dashed-dotted line), the greatest difference (two orders of magnitude) occurring in the low angular momentum region. Therefore, our $(\gamma, 2n)$ isomeric ratio is very sensitive to the identification of the high spin state. Our experimental result $Y_{short}/Y_{long} = 7.7 \pm 2.9$ matches very well the systematic trend of the $(\alpha, 2n)$ and $(d, 2n)$ data in the context of the statistical model and corroborates the conclusion of Ref. 11 that the long-lived state is the high spin state.

Unfortunately the yield ratios calculated within the statistical formalism[28,29] strongly depend on the adopted spin cutoff parameter σ of the spin dependent level density. In Fig. 3 a value of $3\hbar$ was assumed; 3 to $5\hbar$ was used as a reasonable range of σ values in Ref. 11. In Fig. 4 the calculated yield ratios Y_{low}/Y_{high} for the $(\gamma, 2n)$ reaction are plotted as a function of σ for different spin com-

TABLE III. Comparison with previous results from particle induced reactions.

	$T_{1/2}$ (ns)	Reaction	Method	Ref.
Short–lived component	≈60	$(\alpha, 2n)$	R [a]	5
	100 ± 30	$(d, 2n)$	R	9
	120 ± 50	$(\alpha, 2n)$	P [b]	10
	100 ± 50	$(\alpha, 2n)$	P	7
	120 ± 50	(α, n)	P	7
	82 ± 8	$(\alpha, 2n)$	P	11
	88 ± 35 [d]	$(d, 2n)$, $(\alpha, 2n)$	P	11
	114 ± 12	$(d, 2n)$	P	6
	45 ± 10	$(\alpha, 2n)$	P	13
	110 ± 9	$(\alpha, 2n)$	P	14
	77 ± 16 [c]	$(\gamma, 2n)$	P	this work
Long–lived component	900 ± 150	$(d, 2n)$	P	8
	1120 ± 80 [d]	$(\alpha, 2n)$, $(d, 2n)$	P	11
	950 ± 300	$(d, 2n)$	P	6
	1310 ± 260	$(d, 2n)$	P	14
	1050 ± 400	$(\gamma, 2n)$	P	this work

[a] Recoil techniques.
[b] Pulsed beam techniques.
[c] Weighted average of short and long beam pulse experiments.
[d] Weighted average of $(d, 2n)$ and $(\alpha, 2n)$ results.

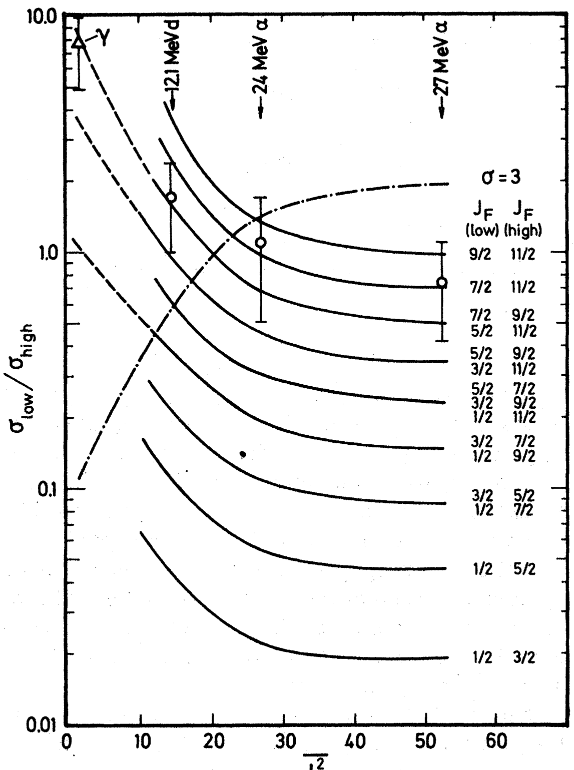

FIG. 3. Theoretical isomeric yield ratios for different final spin combinations in ^{237}Pu as a function of the mean square initial compound nuclear spin $\overline{J_c^2}$. Solid lines: Vandenbosch's calculations (Ref. 11) for $\sigma = 3\hbar$. Dashed lines: extrapolation to small $\overline{J_c^2}$ using our (γ, xn) program (Ref. 30). Dashed-dotted line: calculated isomeric ratio for reversed spin assignment $(\frac{5}{2}-\frac{11}{2})$. Open circles: experimental ratio $\sigma_{short}/\sigma_{long}$ from $(d, 2n)$ and $(\alpha, 2n)$ experiments (Ref. 11). Triangle: $(\gamma, 2n)$ isomeric ratio Y_{short}/Y_{long}.

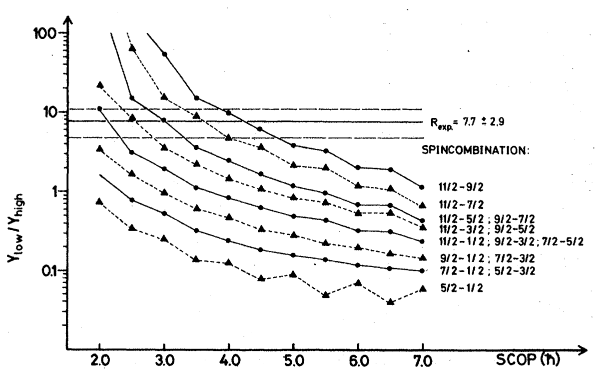

FIG. 4. Theoretical calculation of Y_{low}/Y_{high} as a function of the spin-cutoff parameter (SCOP) for different spin combinations.

binations of the ^{237}Pu fission isomers. Within the statistical model and restricting ourselves to the same σ range ($3-5\hbar$) as in Ref. 11, four probable spin combinations $\frac{11}{2}-\frac{9}{2}$, $\frac{11}{2}-\frac{7}{2}$, $\frac{11}{2}-\frac{5}{2}$, and $\frac{9}{2}-\frac{7}{2}$ can be derived from the comparison of the calculated yield ratios with our experimental ratio $R = 7.7 \pm 2.9$. From life-time arguments the spin pairs $\frac{9}{2}-\frac{7}{2}$, $\frac{11}{2}-\frac{7}{2}$, and $\frac{11}{2}-\frac{9}{2}$ can be excluded as possible candidates for the isomeric pair in ^{237}Pu. Owing to the small multipolarities of the γ transitions for these spin combinations (dipole and quadrupole radiation), the γ-transition lifetime of the upper, high spin level would be too small as compared with the observed half-life of 1100 ns. Therefore this first analysis provides as the most probable spin assignment the spin $I = \frac{11}{2}$ to the long-lived, energetically higher isomer and $I = \frac{5}{2}$ to the ground state in the second minimum of ^{237}Pu.

The results of this analysis are valid only in the context of the statistical model and its approximations. Besides the uncertainty of the choice of the spin cutoff parameter σ, a very simple model is used to describe the γ-deexcitation cascades after the neutron evaporation. Only $E1$ γ transitions were assumed, feeding states differing in spin by $0\hbar$ or $\pm 1\hbar$ from that of the original level. This crude approximation, neglecting collective $E2$ transitions toward lower spin states, clearly overestimates the population of high spin states.

Since no level scheme in the second well is known so far, no reasonable refinement of the deexcitation model seemed to be possible, i.e., $E2$ contributions could not be taken into account without introducing a new arbitrary parameter into the model. Therefore, a more phenomenological approach was attempted. In the past, we had per-

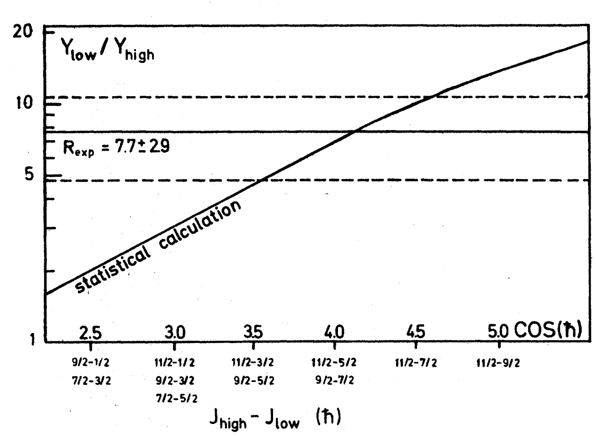

FIG. 5. Theoretical calculation of Y_{low}/Y_{high} using the empirical correlation between spin cutoff parameter (SCOP) and the center of spins (COS); $R_{exp} = Y_{short}/Y_{long}$ from this work.

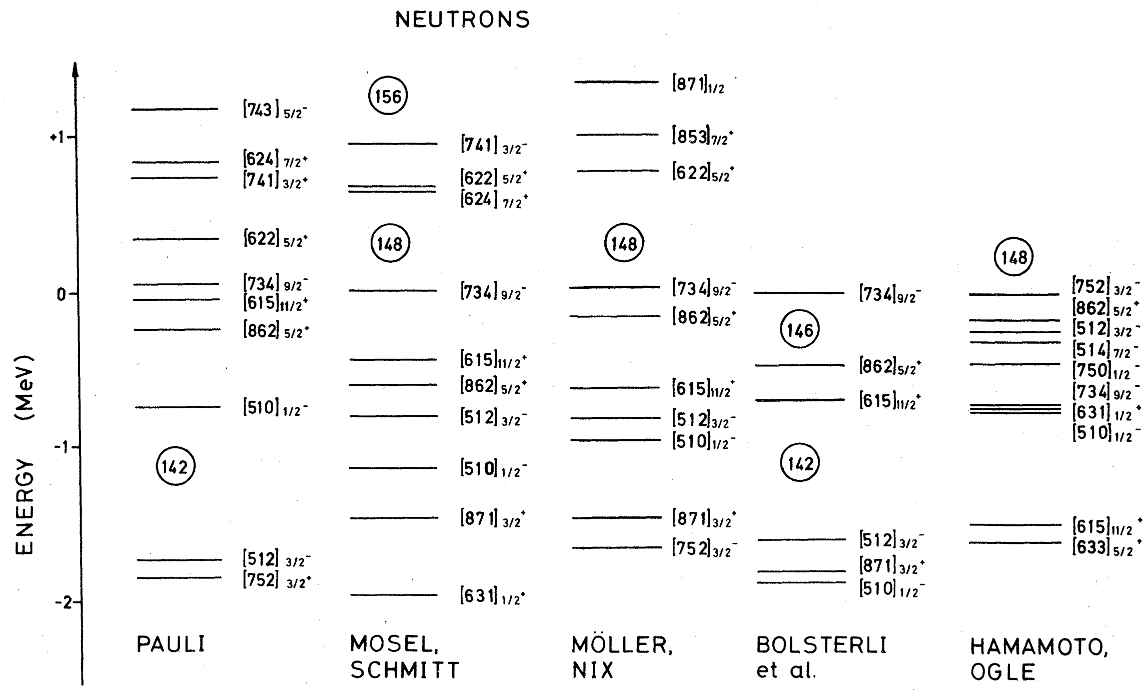

FIG. 6. Single particle energy levels calculated for neutrons at a deformation corresponding to the second minimum in the potential energy surface.

formed a systematic analysis of all available photonuclear (γ, xn) isomeric cross section ratio measurements for isomers with known spins.[30,32] This analysis showed a linear correlation between spin cutoff parameters (σ) derived by the simple statistical model[28,29] and the mean value of the spins of the isomeric pair (COS). If we, vice versa, use this empirical correlation between σ and the mean spin value for spin assignments, we indirectly take into account the shortcomings of the model. Using this linear correlation (fitted from all experimental σ values summarized in Ref. 32) and the calculation shown in Fig. 4 the yield ratio $Y_{\text{low}}/Y_{\text{high}}$ only depends on the mean spin value (COS) (see Fig. 5). The line of intersection between the calculated curve (labeled statistical calculation) and the shaded area of the experimental yield ratio provides as the most probable COS value $4\hbar$, and with less probability 3.5 and $4.5\hbar$, which cannot be excluded definitely (see Fig. 5). Since spin combinations with spin differences $\leq 2\hbar$ again can be excluded by lifetime arguments, $\frac{11}{2}-\frac{5}{2}$ remains as the most probable spin combination also in this modified analysis. This assignment fully agrees with the conclusions of Vandenbosch *et al.*[11] based on the $(\alpha, 2n)$ and $(d, 2n)$ isomeric ratios.

In Fig. 6 neutron single particle levels are plotted, which were calculated by Pauli *et al.*,[20] Mosel and Schmitt,[21] Möller and Nix,[22] Bolsterli *et al.*,[23] and Hamamoto *et al.*[15] with different potential approaches. All level schemes, except the Hamamoto calculation, show the $[615]_{11/2^+}$ and $[862]_{5/2^+}$ Nilsson orbitals at the Fermi surface for ^{237}Pu (143 neutrons). The 143rd neutron presumably should be expected in a $\frac{11}{2}^+$ or $\frac{5}{2}^+$ state. An exact ordering of the states would be fortuitous. However, the systematic trend of the ^{237}Pu isomeric yield ratio measurements tends to indicate that the long-lived, energetically higher isomer in ^{237}Pu is the $[615]_{11/2^+}$ Nilsson state and the short-lived ground state in the second well is the $[862]_{5/2^+}$ state. This is in disagreement with the suggestions of Hamamoto *et al.*,[15] based on the *g* factor and angular distribution measurements of Kalish *et al.*[16,17] It is possible that the favored spin assignments of $[514]_{7/2^-}$ and $[512]_{3/2^-}$ from the latter work[16,17] could be a consequence of experimental problems, and that the unusually strong spin-orbit strength explains the displacement of the $[615]_{11/2^+}$ and $[862]_{5/2^+}$ orbitals from the vicinity of the Fermi surface in the calculations of Hamamoto *et al.*[15]

We would like to thank Professor U. Mosel for his interest and fruitful discussions. We are indebted to Professor H. J. Specht for stimulating discussions and helpful comments. Thanks are due to Dipl. Phys. H. O. Neidel and S. Schulz for their help during the experiments. We also thank the Giessen linac staff for the excellent machine maintenance. Financial support of the Deutsche Forschungsgemeinschaft is gratefully acknowledged. This paper is part of a thesis (D26, H. K.)

---

[1]H. J. Specht, J. Weber, E. Konecny, and D. Heunemann, Phys. Lett. 41B, 43 (1972).
[2]D. Habs, V. Metag, H. J. Specht, and G. Ulfert, Phys. Lett. 38, 387 (1977).
[3]V. M. Strutinsky, Nucl. Phys. A95, 420 (1967).
[4]V. M. Strutinsky, Nucl. Phys. A122, 1 (1968).
[5]V. Metag, R. Repnow, P. von Brentano, and J. D. Fox, Z. Phys. 226, 1 (1969).
[6]J. K. Temperley, J. A. Morrissey, and S. L. Bacharach, Nucl. Phys. A175, 443 (1971).
[7]H. C. Britt, S. C. Burnett, B. H. Erkkila, J. E. Lynn, and W. E. Stein, Phys. Rev. C 4, 1444 (1971).
[8]S. M. Polikanov, G. Sletten, Nucl. Phys. A151, 656 (1970).
[9]N. L. Lark, G. Sletten, J. Pedersen and S. Bjørnholm, Nucl. Phys. A139, 481 (1969).
[10]S. C. Burnett, H. C. Britt, B. H. Erkkila, and W. E. Stein, Phys. Lett. 31B, 529 (1970).
[11]P. A. Russo, R. Vandenbosch, M. Mehta, J. R. Tesmer, and K. L. Wolf, Phys. Rev. C 3, 1595 (1971).
[12]R. Vandenbosch, P. A. Russo, G. Sletten, and M. Mehta, Phys. Rev. C 8, 1080 (1973).
[13]H. J. Specht, E. Konecny, J. Weber, and C. Kozhuharov, in *Proceedings of the Conference on Physics and Chemistry of Fission* (IAEA, Vienna, 1973), Vol. 1, 285.
[14]S. L. Bacharach, P. S. Hoeper, J. A. Morrissey, and J. K. Temperley, Phys. Rev. C 10, 2636 (1974).
[15]I. Hamamoto and W. Ogle, Nucl. Phys. A240, 54 (1975).
[16]R. Kalish, B. Herskind, J. Pedersen, D. Shackleton, and L. Strabo, Phys. Rev. Lett. 32, 1009 (1974).
[17]D. Shackleton, B. Herskind, R. Kalish, J. Pedersen, and L. Strabo, in *Proceedings of the International Conference on Hyperfine Interactions studied in Nuclear Reactions and Decay, Uppsala, Sweden, 1974*, edited by E. Karlsson and R. Wäppling (Upplands Grafiska, AB, Uppsala, 1974).
[18]H. J. Specht, private communication.
[19]R. Vandenbosch, Annu. Rev. Nucl. Sci. 27, 1 (1977).
[20]H. C. Pauli, Phys. Rev. C 7, 35 (1973).
[21]U. Mosel and H. W. Schmitt, Nucl. Phys. A165, 13 (1971).
[22]P. Möller and J. R. Nix, in *Proceedings of the Conference on Physics and Chemistry of Fission* (IAEA, Vienna, 1973), Vol. 1, 103.
[23]M. Bolsterli, E. O. Fiset, J. R. Nix, and J. L. Norton, Phys. Rev. C 5, 1050 (1972).
[24]H. Bartsch, W. Günther, K. Huber, U. Kneissl, H. Krieger, and H. J. Maier, Nucl. Phys. A306, 29 (1978).
[25]W. Günther, K. Huber, U. Kneissl, and H. Krieger, Nucl. Phys. A297, 254 (1978).
[26]H. Bartsch, K. Huber, U. Kneissl, and H. Sattler, Nucl. Instrum. Methods 121, 185 (1974).
[27]B. Tamain, B. Pfeiffer, H. Wollnik, and E. Konecny, Nucl. Phys. A173, 465 (1971).
[28]J. R. Huizenga and R. Vandenbosch, Phys. Rev. 120, 1305 (1960).
[29]R. Vandenbosch and J. R. Huizenga, Phys. Rev. 120, 1313 (1960).
[30]H. Bartsch, K. Huber, U. Kneissl, and H. Krieger, Nucl. Phys. A256, 243 (1976).
[31]P. Limkilde and G. Sletten, Nucl. Phys, A199, 504 (1973).
[32]H. Bartsch, W. Günther, K. Huber, U. Kneissl, and H. Krieger, Z. Phys. A285, 71 (1978).